Visualization of Vortex Bound States in Polarized Fermi Gases at Unitarity

Hui Hu,[1,2] Xia-Ji Liu,[2] and Peter D. Drummond[2]

[1]*Department of Physics, Renmin University of China, Beijing 100872, China*
[2]*ARC Centre of Excellence for Quantum-Atom Optics, Department of Physics, University of Queensland, Brisbane, Queensland 4072, Australia*

(Received 15 August 2006; published 8 February 2007)

We theoretically analyze a single vortex in a spin polarized 3D trapped atomic Fermi gas near a broad Feshbach resonance. Above a critical polarization the Andreev-like bound states inside the core become occupied by the majority spin component. As a result, the local density difference at the core center suddenly rises at low temperatures. This provides a way to visualize the lowest bound state using phase-contrast imaging. As the polarization increases, the core expands gradually and the energy of the lowest bound state decreases.

DOI: 10.1103/PhysRevLett.98.060406 PACS numbers: 05.30.Fk, 03.75.Ss, 67.90.+z, 74.20.−z

The achievement of superfluidity in trapped ultracold atomic ^{6}Li gases is a landmark advance in the history of physics [1]. This is attained by utilizing a broad Feshbach resonance, which is used to tune the interatomic interactions. By changing the inverse scattering length a_s continuously from negative to positive values, a two-component Fermi gas with *equal* spin populations has a ground state which crosses smoothly from Bardeen-Cooper-Schrieffer (BCS) superfluidity to a Bose-Einstein condensate (BEC) of tightly bound pairs. Of particular interest is the unitarity regime near resonance, where the scattering length diverges ($1/a_s \simeq 0$). Since the interparticle spacing is the only relevant length scale, the Fermi gas exhibits a universal behavior [2].

Quantized vortices are a clear-cut confirmation of superfluidity, and were demonstrated experimentally by Zwierlein *et al.* [1]. The equilibrium properties of vortices in a symmetric Fermi superfluid at crossover have been the subject of intense theoretical studies [3–9]. The Andreev-like bound states, which are the fermionic quasiparticle excitations localized in the core, have been widely discussed [3,6,8,9]. These bound states are found to play a key role in the structure of vortices.

Most recently, Fermi gases with *unequal* spin populations have been the subject of considerable experimental [10,11] and theoretical interest [12–18]. The presence of spin polarization leads to exotic forms of pairing, such as breached pairing [12] or Sarma superfluidity [13], phase separation [14], and spatially modulated Fulde-Ferrell-Larkin-Ovchinnikov (FFLO) states [15]. An agreement on the *true* ground state of polarized fermionic superfluidity is yet to be reached. However, three recent measurements on the density profiles of polarized ^{6}Li gases [10,11], near a Feshbach resonance, indicate a paired superfluid core surrounded by the excess unpaired fermions consistent with a picture of phase separation.

Combining spin polarization with a vortex may help to resolve the issue of the nature of polarized fermion pairing. It is natural to ask how unequal spin populations affect the vortex structure, and how vortex bound states evolve as the polarization increases. This issue arises in the context of pairing and superfluidity in many fields of physics [19]. It is highly relevant to the condensed matter community, where polarized superfluidity is created by applying a magnetic field. There is now strong experimental evidence for the existence of FFLO states in the heavy fermion superconductor $CeCoIn_5$ under high fields [20]. Strongly interacting polarized Fermi gases have also been under close scrutiny in nuclear matter [21], neutron stars [21], and high density quark matter [19,22], where the spin polarization is created by differences between chemical potentials and/or by mass differences between fermions that form pairs. Polarized vortices of color superfluidity in rotating neutron stars are a possible mechanism for observed glitches in pulsar timing [19].

Here we investigate the properties of a singly quantized vortex in polarized atomic Fermi gases at unitarity, in a cylindrically symmetric trap. Our main results are: (a) we clarify the density profiles of both spin components as a function of polarization. In addition to phase separation, the vortex core suddenly accommodates the excess majority fermions above a critical polarization or a critical chemical potential difference, resulting in a rapid rise of the local density difference inside the core. (b) The local fermionic density of states explains the sudden appearance of an unpaired core of excess majority atoms at the vortex center. The Andreev-like bound states in the core are occupied when the critical chemical potential difference equals the lowest available energy. This provides a clear visualization of vortex bound states using phase-contrast imaging [23]. (c) With increasing polarization, the vortex core expands while the lowest bound state energy decreases.

The above results are obtained by numerically solving the mean-field Bogoliubov–de Gennes (BdG) equations in a fully self-consistent fashion [3,24], assuming a pairing order parameter that preserves the cylindrical and axially translational symmetries. Symmetry breaking is also pos-

sible; i.e., the order parameter may distort cylindrically. This scenario merits further study.

Fermi gases of ^{6}Li atoms near a broad Feshbach resonance are well characterized using a single channel model [25]. The BdG equations describing the quasiparticle wave functions $u_\eta(\mathbf{r})$ and $v_\eta(\mathbf{r})$, with excitation energies E_η read [3]:

$$\begin{bmatrix} \mathcal{H}_0 - \mu_\uparrow & \Delta(\mathbf{r}) \\ \Delta^*(\mathbf{r}) & -\mathcal{H}_0 + \mu_\downarrow \end{bmatrix} \begin{bmatrix} u_\eta(\mathbf{r}) \\ v_\eta(\mathbf{r}) \end{bmatrix} = E_\eta \begin{bmatrix} u_\eta(\mathbf{r}) \\ v_\eta(\mathbf{r}) \end{bmatrix}, \tag{1}$$

where $\mathcal{H}_0 = -\hbar^2\nabla^2/2m + V_{\rm ext}(\mathbf{r})$, and $V_{\rm ext}(\mathbf{r}) = m\omega^2(x^2+y^2)/2$ is the transverse trapping potential. Along the z axis we instead assume free motion over a length L. To account for the unequal spin population N_σ for $\sigma = \uparrow, \downarrow$ the chemical potentials are shifted as $\mu_{\uparrow,\downarrow} = \mu \pm \delta\mu$, leading to different quasiparticle wave functions for the two components. However, there is a symmetry of the BdG equations under the replacement $u^*_{\eta\downarrow}(\mathbf{r}) \to v_{\eta\uparrow}(\mathbf{r})$, $v^*_{\eta\downarrow}(\mathbf{r}) \to -u_{\eta\uparrow}(\mathbf{r})$, $E_{\eta\downarrow} \to -E_{\eta\uparrow}$. We can thus retain only $u_{\eta\uparrow}(\mathbf{r})$ and $v_{\eta\uparrow}(\mathbf{r})$ in Eq. (1), and keep solutions with both positive and negative energies.

The order parameter $\Delta(\mathbf{r})$ and the chemical potentials $\mu_{\uparrow,\downarrow}$ are determined by self-consistency equations for the gap, $\Delta(\mathbf{r}) = g\sum_\eta u_\eta(\mathbf{r})v^*_\eta(\mathbf{r})f(E_\eta)$, and the particle density of each component: $n_\uparrow(\mathbf{r}) = \sum_\eta |u_\eta(\mathbf{r})|^2 f(E_\eta)$ and $n_\downarrow(\mathbf{r}) = \sum_\eta |v_\eta(\mathbf{r})|^2 f(-E_\eta)$. These must be constrained so that $\int d\mathbf{r} n_\sigma(\mathbf{r}) = N_\sigma$, where $f(x) = 1/(e^{x/k_BT}+1)$ is the Fermi distribution function, and g (<0) is the bare coupling constant, which is related to the s-wave scattering length via the regularization prescription: $(4\pi\hbar^2 a_s/m)^{-1} = 1/g + \sum_{\mathbf{k}} 1/2\epsilon_{\mathbf{k}}$.

We solve these equations via a *hybrid* procedure, by introducing a high energy cutoff E_c above which we use a local density approximation (LDA) for high-lying excitation levels. The standard regularization prescription then yields an effective coupling constant through the self-consistency equation $\Delta(\mathbf{r}) = g_{\rm eff}(\mathbf{r})\sum'_\eta u_\eta(\mathbf{r})v^*_\eta(\mathbf{r})f(E_\eta)$, where the cutoff summation $\sum'_\eta$ is now restricted to $|E_\eta| \le E_c$. Further details of this will be given elsewhere. A clear limitation of the procedure is the use of mean-field factorizations implicit in the BdG equations. From earlier work, we expect this to neglect quantum fluctuations that alter the ground-state energy, while remaining qualitatively correct [26].

Below the cutoff, we solve the BdG equations by working in cylindrical coordinates (ρ, φ, z) and taking $\Delta(\mathbf{r}) = \Delta(\rho)e^{-i\varphi}$ for a singly quantized vortex. Assuming periodic boundary conditions at $z = \pm L/2$, we write, for the normalized modes, $u_\eta(\mathbf{r}) = u_{nmk_z}(\rho)e^{im\varphi}e^{ik_z z}/\sqrt{2\pi L}$ and $v_\eta(\mathbf{r}) = v_{nmk_z}(\rho)e^{i(m+1)\varphi}e^{ik_z z}/\sqrt{2\pi L}$ with $k_z = 2\pi l/L$. As a consequence, the BdG equations decouple into different m and l sectors [3]. Expanding the radial functions $u_{nmk_z}(\rho)$ and $v_{nmk_z}(\rho)$ in a basis set of 2D harmonic oscillators, we then solve a matrix eigenvalue problem in each sector.

In greater detail, we consider a gas at unitarity with the number of total atoms in the range $N = N_\uparrow + N_\downarrow = 2\times 10^3 - 4\times 10^4$. Two characteristic scales may be defined by considering a symmetric ideal Fermi gas at zero temperature. In the LDA analysis this leads to a Thomas-Fermi (TF) radius $\rho^0_{\rm TF} = (15\pi N\lambda/2)^{1/6}\sqrt{\hbar/m\omega}$, and a Fermi energy $E_F = (15\pi N\lambda/16)^{1/3}\hbar\omega \equiv k_B T_F$, where we define $\lambda = L/\rho^0_{\rm TF}$ as the aspect ratio of the trap. Throughout this Letter, we calculate results at the Feshbach resonance with $1/a_s = 0$ and use $\lambda = 1$ and $E_c \simeq 2E_F$. We also considered coupling constants in the BCS regime but observed no significant changes. Dimensionality effects will be treated elsewhere.

Numerical accuracy was checked by increasing E_c up to $4E_F$. Because of the high accuracy of our hybrid cutoff procedure, the results were found to be essentially independent of the cutoff energy. We note finally that, for a symmetric gas at unitarity, universality implies a TF radius of $\rho_{\rm TF} = (1+\beta)^{3/10}\rho^0_{\rm TF}$, a chemical potential $\mu = (1+\beta)^{3/5}E_F$, and a maximum order parameter $\Delta_0 = 8(1+\beta)^{3/5}E_F/e^2$ [2], where BCS theory predicts the universal parameter $\beta \simeq -0.41$.

We present in Figs. 1(a)–1(c) the density profile of each component, as well as the density difference $\delta n(\mathbf{r}) = n_\uparrow(\mathbf{r}) - n_\downarrow(\mathbf{r})$, for several polarizations $p = (N_\uparrow - N_\downarrow)/N$ at $T = 0.05T_F$ and $N = 10^4$. Because of the uniform distribution along the z axis, these profiles are linked to the experimentally observed column densities in the axial

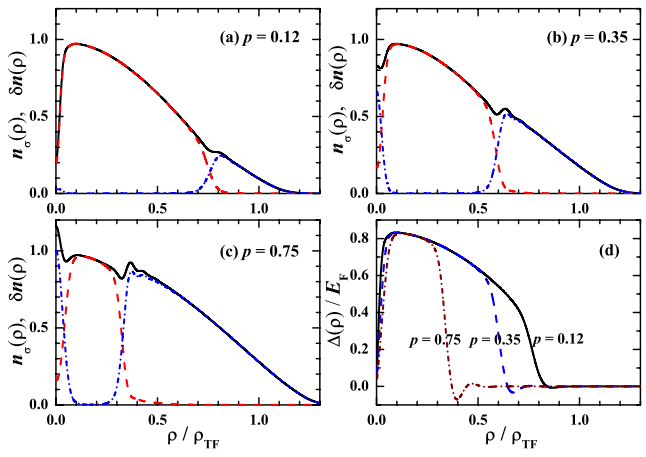

FIG. 1 (color online). Density profiles of the majority ($\uparrow$ state, solid lines) and minority ($\downarrow$ state, dashed lines) components at $T = 0.05T_F$ for three typical value of polarization: $p = 0.12$ (a), $p = 0.35$ (b), and $p = 0.75$ (c). Density differences are also plotted in dot-dashed lines. All the profiles are normalized by $n_{\sigma,\rm TF} = (1+\beta)^{-3/5}\sqrt{15\pi N\lambda/2}/(6\pi^2)(\hbar/m\omega)^{-3/2}$, which is the peak density for a symmetric gas at unitarity. Panel (d) shows the order parameter profiles. The small oscillations at the edge are a finite size effect.

direction. Apart from the apparent phase separation at the edge, the most salient feature of the figures is the development of a polarized normal shell inside the vortex core above a certain polarization. This is clearly visible as a prominent peak in the density difference, of width about $0.05\rho_{\mathrm{TF}}$. This is observable in the column integrated density difference, which is directly measurable by phase-contrast imaging [10,23].

The onset of a polarized normal shell at the core center is demonstrated by the central density difference as a function of the polarization. This is shown in Fig. 2(a), which represents the most important result of this Letter. At a sufficiently low temperature, i.e., $T = 0.01T_F$, a sudden rise of the center density difference appears at a critical polarization $p_c \simeq 0.30$. The critical chemical potential difference is $\delta\mu_c \simeq 0.36E_F \sim \Delta_0^2/2E_F$, with a transition width of around k_BT. This transition is therefore much smoother at finite temperature. The critical polarization is nearly independent of the overall number of atoms N, as shown in Fig. 2(b) for N up to 4×10^4. We therefore expect that this will apply to current experiments, where the typical number of atoms is around 10^5, and would survive even in the thermodynamic limit.

The appearance of this intriguing shell structure is closely related to the Andreev-like bound states inside the core. In the BCS regime, these states are formed by the spatial variation of the order parameter around the center [see, i.e., Fig. 1(d)], analogous to a potential well for quasiparticles, of depth Δ_0 and of radius equal to the coherence length $\xi = \hbar v_F/\Delta_0$. Hence, the confinement of the well gives rise to discrete bound levels with spacing of order $\hbar^2/m\xi^2 = \Delta_0^2/2E_F$ [3]. This qualitative picture persists in the strongly interacting unitarity limit [9].

To provide an intuitive explanation of our results, we calculate the local density of states (LDOS),

$$N_\uparrow(\mathbf{r}, E) = \sum_\eta |u_\eta(\mathbf{r})|^2 \delta(E - E_\eta),$$
$$N_\downarrow(\mathbf{r}, E) = \sum_\eta |v_\eta(\mathbf{r})|^2 \delta(E + E_\eta). \quad (2)$$

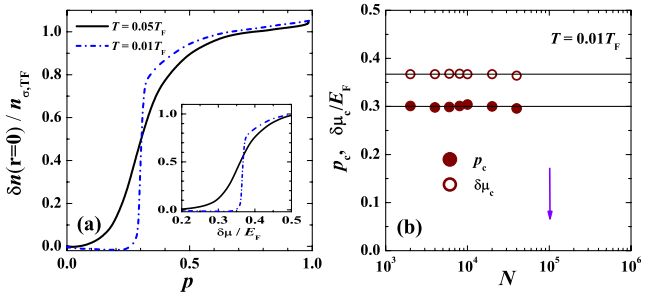

FIG. 2 (color online). Left panel: center density difference as a function of polarization at $N = 10^4$. Inset shows the dependence on the chemical potential difference. Right panel: critical polarization and critical chemical difference as a function of the number of total particles.

At low temperature, when integrated over negative energy, this leads to the density profiles $n_\sigma(\mathbf{r})$. In Fig. 3 we show how the LDOS inside the core evolves with increasing the polarization. A small spectral broadening of about $0.01E_F$ has been used to regularize the delta function. Without any polarization the LDOS of the two components coincides, leading to a sharp peak located at positive energy $E_{\mathrm{bs}}^0 \simeq \Delta_0^2/2E_F$, associated with the lowest Andreev-like bound state.

In the presence of spin-polarization the peak in the density of states shifts in different directions for the two components. To a good approximation, the energy separation between the two peaks at the vortex center equals $2\delta\mu$. Thus, in the general case of a nonzero polarization one may define an effective energy of the lowest bound state, E_{bs}, as the midpoint of these two peaks located at $E_{\mathrm{bs}} \mp \delta\mu$. Therefore, a net density difference results precisely when the peak in $N_\uparrow(\mathbf{r} = \mathbf{0}, E)$ crosses zero energy, i.e., $\delta\mu = E_{\mathrm{bs}}$. This results in a bound state for the majority spin component, which explains why a polarized normal shell emerges above a critical population chemical potential $\delta\mu_c \sim E_{\mathrm{bs}}^0 \simeq \Delta_0^2/2E_F$.

Thus, the integrated column density difference is an indicator of the lowest vortex bound state, and a measurement of the critical polarization p_c gives its energy.

We now consider the dependence of the vortex core size on the polarization. We extract the core size from the superfluid density $n_s(\mathbf{r})$, defined as a ratio of the current density $\mathbf{j}(\mathbf{r}) = n_s(\mathbf{r})\mathbf{v}_s$ to the superfluid velocity $\mathbf{v}_s = (\hbar/2m\rho)\hat{\varphi}$ [9], where, since our normal fluid solutions are nonrotating:

$$\mathbf{j}(\mathbf{r}) = \frac{i\hbar}{m\rho}\sum_\eta [u_\eta^* \partial_\varphi u_\eta f(E_\eta) + v_\eta \partial_\varphi v_\eta^* f(-E_\eta)]\hat{\varphi}. \quad (3)$$

The resulting superfluid density profiles are plotted in the inset of Fig. 4(a). The core size may be quantified as the distance from the vortex core at which the superfluid density is 90% of its maximum value, namely, ξ_{90}. From Fig. 4(a), the core size increases gradually with increasing polarization, and almost doubles at large polarization.

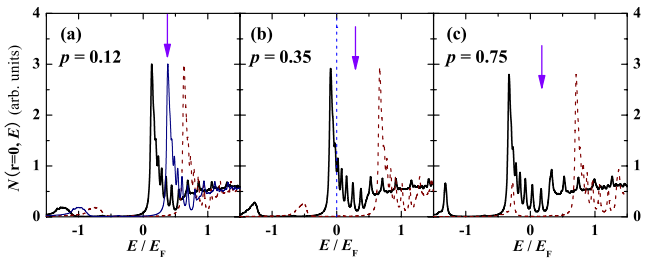

FIG. 3 (color online). Local fermionic density of states of spin-up (solid lines) and spin-down (dashed lines) components inside the vortex core at $N = 10^4$ and $T = 0.05T_F$. The thin line in (a) shows the LDOS at $p = 0$. Arrows point to the position at the effective energy of the lowest bound state.

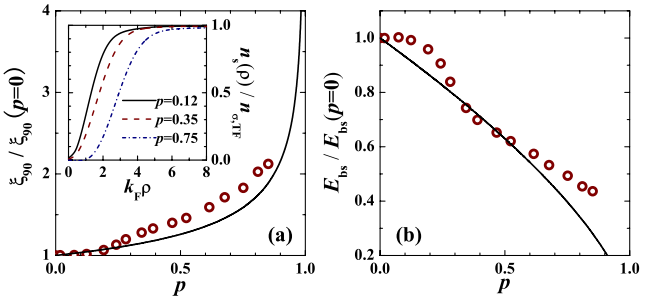

FIG. 4 (color online). Vortex core size (a) and the effective energy of the lowest bound state (b) as a function of polarization at $N = 10^4$ and $T = 0.05T_F$. The core size ξ_{90} at $p = 0$ is about $2.5k_F^{-1}$, where k_F noninteracting Fermi wavelength at center. Solid lines are the scaling relations as described in the text. Inset shows superfluidity density profiles.

To explain this, note that while a phase separation occurs at *any* nonzero polarization, only the unpolarized superfluid part can form a vortex. Thus, the vortex core should expand with a scaling of $\xi_{90} \propto (2N_\downarrow)^{-1/3} \propto (1-p)^{-1/3}$ [9]. In Fig. 4(a) this scaling is plotted by a solid line, which fits well with our numerical results. Accordingly, one may suspect that the energy of the lowest bound state will decrease as $E_{\rm bs} \propto 1/\xi_{90}^2 \propto (1-p)^{2/3}$. This is consistent with the effective energy of the lowest bound state shown in Fig. 4(b). We expect a phase separation into *multiple* vortex cores in a vortex lattice, as in current nonpolarized experiments [1].

We have considered an aspect ratio $\lambda = 1$, which is closer to the MIT experimental setup [10] than the Rice experiment (which has $\lambda = 50$ [11]). In the opposite limit of $\lambda \ll 1$, an interesting aspect of dimensionality would arise. Because of strong phase fluctuations, this quasi-2D geometry would favor the spontaneous formation of vortices at finite temperature [27]. As a result, a lattice of vortex-antivortex pairs *without* phase separation may emerge as the ground state. In such a configuration, the spin polarization would be sustained by a polarized normal shell *inside* the vortex cores, analogous to a type-II superconductor in a magnetic field.

In conclusion, we have analyzed vortex structures in a polarized Fermi gas at unitarity. The lowest bound state will be visible via phase-contrast imaging, together with a quantum phase transition at a critical spin polarization.

This work is supported by the Australian Research Council Center of Excellence program and by the National Science Foundation of China under Grant No. NSFC-10574080 and the National Fundamental Research program under Grant No. 2006CB921404. One of us (P. D. D.) acknowledges useful discussions with Yong-Il Shin.

[1] M. W. Zwierlein *et al.*, Nature (London) **435**, 1047 (2005).
[2] T.-L. Ho, Phys. Rev. Lett. **92**, 090402 (2004).
[3] F. Gygi and M. Schlüter, Phys. Rev. B **43**, 7609 (1991).
[4] N. Nygaard *et al.*, Phys. Rev. Lett. **90**, 210402 (2003).
[5] A. Bulgac and Y. Yu, Phys. Rev. Lett. **91**, 190404 (2003).
[6] M. Machida and T. Koyama, Phys. Rev. Lett. **94**, 140401 (2005).
[7] T. Mizushima, K. Machida, and M. Ichioka, Phys. Rev. Lett. **95**, 117003 (2005).
[8] C.-C. Chien *et al.*, Phys. Rev. A **73**, 041603(R) (2006).
[9] R. Sensarma, M. Randeria, and T.-L. Ho, Phys. Rev. Lett. **96**, 090403 (2006).
[10] M. W. Zwierlein *et al.*, Science **311**, 492 (2006); Nature (London) **442**, 54 (2006).
[11] G. B. Partridge *et al.*, Science **311**, 503 (2006).
[12] W. V. Liu and F. Wilczek, Phys. Rev. Lett. **90**, 047002 (2003).
[13] G. Sarma, J. Phys. Chem. Solids **24**, 1029 (1963); C.-H. Pao, S.-T. Wu, and S.-K. Yip, Phys. Rev. B **73**, 132506 (2006).
[14] P. F. Bedaque, H. Caldas, and G. Rupak, Phys. Rev. Lett. **91**, 247002 (2003).
[15] P. Fulde and R. A. Ferrell, Phys. Rev. **135**, A550 (1964); A. I. Larkin and Y. N. Ovchinnikov, Zh. Eksp. Teor. Fiz. **47**, 1136 (1964) [Sov. Phys. JETP **20**, 762 (1965)].
[16] H. Müther and A. Sedrakian, Phys. Rev. Lett. **88**, 252503 (2002); J. Carlson and S. Reddy, Phys. Rev. Lett. **95**, 060401 (2005); L. He, M. Jin, and P. Zhang, Phys. Rev. B **73**, 214527 (2006); T.-L. Ho and H. Zhai, cond-mat/0602568.
[17] D. T. Son and M. A. Stephanov, Phys. Rev. A **74**, 013614 (2006); D. E. Sheehy and L. Radzihovsky, Phys. Rev. Lett. **96**, 060401 (2006); K. Yang, cond-mat/0508484; H. Hu and X.-J. Liu, Phys. Rev. A **73**, 051603(R) (2006).
[18] J. Kinnunen, L. M. Jensen, and P. Törma, Phys. Rev. Lett. **96**, 110403 (2006); F. Chevy, Phys. Rev. Lett. **96**, 130401 (2006); W. Yi and L.-M. Duan, Phys. Rev. A **73**, 031604 (2006); T. N. De Silva and E. J. Mueller, Phys. Rev. A **73**, 051602(R) (2006); M. Haque and H. T. C. Stoof, Phys. Rev. A **74**, 011602(R) (2006); A. Imambekov *et al.*, Phys. Rev. A **74**, 053626 (2006).
[19] For a review, see, for example, R. Casalbuoni and G. Nardulli, Rev. Mod. Phys. **76**, 263 (2004).
[20] H. A. Radovan *et al.*, Nature (London) **425**, 51 (2003); C. F. Miclea *et al.*, Phys. Rev. Lett. **96**, 117001 (2006).
[21] A. Sedrakian and J. W. Clark, nucl-th/0607028.
[22] M. Alford and K. Rajagopal, hep-ph/0606157.
[23] Y. Shin *et al.*, Phys. Rev. Lett. **97**, 030401 (2006).
[24] P. G. de Gennes, *Superconductivity of Metals and Alloys* (Addison-Wesley, Reading, MA, 1989).
[25] R. Diener and T.-L. Ho, cond-mat/0405174; X.-J. Liu and H. Hu, Phys. Rev. A **72**, 063613 (2005).
[26] H. Hu, X.-J. Liu, and P. D. Drummond, Europhys. Lett. **74**, 574 (2006); Phys. Rev. A **73**, 023617 (2006).
[27] S. S. Botelho and C. A. R. Sá de Melo, Phys. Rev. Lett. **96**, 040404 (2006).